Article

Radio-Protective Effects of Ultra-Fine Bubble Hydrogen Water and Serum Protein Responses in Whole-Body Radiation-Exposed Mice

Masaru Yamaguchi , Khin Thandar Htun , Youta Tatara , Yoshiaki Sato , Masato Hosoda , Suchart Kothan , Chikashi Kamimura , Osamu Inanami , Ikuo Kashiwakura *

Posted Date: 1 August 2024

doi: 10.20944/preprints202408.0106.v1

Keywords: Ultra-fine bubble hydrogen water, Whole body irradiation, Radio-protective effects, Proteome analysis, Scavenging ability against hydroxy radicals

Article

Radio-Protective Effects of Ultra-Fine Bubble Hydrogen Water and Serum Protein Responses in Whole-Body Radiation-Exposed Mice

Masaru Yamaguchi [1§], Khin Thandar Htun [2§], Youta Tatara [3], Yoshiaki Sato [4], Masato Hosoda [5], Suchart Kothan [2], Chikashi Kamimura [6], Osamu Inanami [7], Ikuo Kashiwakura[1*]

[1] Graduate School of Health Sciences, Hirosaki University, 66-1 Hon-cho, Hirosaki, Aomori 036-8564, Japan; masarun@hirosaki-u.ac.jp (M.Y.), ikashi@hirosaki-u.ac.jp (I.K.)
[2] Center of Radiation Research and Medical Imaging, Department of Radiologic Technology, Faculty of Associated Medical Sciences, Chiang Mai University, Chiang Mai 50200, Thailand; ktdhtun28@gmail.com (K.T.H), suchart.kothan@cmu.ac.th (S.K.)
[3] Graduate School of Medicine, Hirosaki University, 5 Zaifu-cho, Hirosaki, Aomori 036-8562, Japan; ytatara@hirosaki-u.ac.jp (Y.T.)
[4] Norris Comprehensive Cancer Center, University of Southern California, 1450 Biggy Street, NRT Rm 4516, Los Angeles, CA 90033, USA; yoshiaki@usc.edu (Y.S.)
[5] Interprotein Corporation, Osaka 531-0072, Japan; hosoda@interprotein.com (M.H.)
[6] Information Science Research Institute Ltd., 535-3 Mohno, Ueki-cho, Kita-ku, Kumamoto, Kumamoto, 861-0134, Japan; info@alk-inc.co.jp (C.K.)
[7] Laboratory of Radiation Biology, Department of Applied Veterinary Sciences, Faculty of Veterinary Medicine, Hokkaido University, Sapporo, Japan; inanami@vetmed.hokudai.ac.jp (O.I.)
* Correspondence: ikashi@hirosaki-u.ac.jp
§ These authors have made an equivalent contribution to the first author.

Abstract: Many studies have demonstrated hydrogen's therapeutic and preventive effects on various diseases. Its selective antioxidant properties against hydroxyl radicals, which are responsible for the indirect effects of ionizing radiation, may make it worthy of attention as a new radio-protector. We recently developed new hydrogen water that is more stable and has higher antioxidant activity by using ultra-fine bubbles. In this study, female C57BL/6J mice given *ad libitum* access to ultra-fine bubble hydrogen water (UBHW) were subjected to whole-body irradiation (WBI) with X-rays, and the radio-protective effect of UBHW was evaluated. Sub-lethal WBI resulted in a 30-day survival rate of 100% in UBHW-fed mice, compared with 37% in control mice. In the case of lethal WBI, while the control mice died out in about 3 weeks, the 30-day survival rate improved to 40% by UBHW due to the high scavenging activity of hydroxy radicals. Twenty-six serum proteins involved in inflammatory and immune responses were significantly identified in UBHW-fed mice by proteomics, and UBHW may enhance and regulate these functions, resulting in reduced damage in mice exposed to WBI. We conclude that UBHW has good potential in radio-protection, with evidence that warrants further research efforts in this field.

Keywords: ultra-fine bubble hydrogen water; whole body irradiation; radio-protective effects; proteome analysis; scavenging ability against hydroxy radicals

1. Introduction

The main biological effects of ionizing radiation can be broadly divided into direct effects, in which radiation cleaves the target molecule DNA, and indirect effects, in which reactive oxygen species (ROS) and free radicals, such as hydroxy radical (•OH), superoxide anion ($O_2^{\bullet-}$) and hydrogen peroxide (H_2O_2) generated by ionizing and exciting water molecules in the organism are involved [1, 2]. About 70% of these are caused by indirect effects. Among the molecular species of ROS and free radicals, hydroxy radicals are the most reactive, nonspecifically oxidizing and modifying nucleic acids, proteins, and lipids, and exerting toxicity.

 doi:10.20944/preprints202408.0106.v1

Molecular hydrogen is an antioxidant that diffuses easily *in vivo* and selectively reduces highly toxic radicals. Ohsawa *et al*. reported that inhalation of hydrogen gas could alleviate cerebral ischemia-reperfusion injury [3]. They showed that hydrogen is an antioxidant, selectively reducing the highly oxidizing hydroxy radicals, and peroxynitrite ($ONOO^-$) formed by the direct reaction of superoxide anion and nitric oxide (NO), respectively, but does not react with other ROS such as superoxide anion or hydrogen peroxide. Subsequently, a wide range of applications of hydrogen gas therapy has been reported in clinical and preclinical studies, including brain diseases, inflammatory bowel diseases, and vascular diseases [4-8]. Furthermore, as hydrogen reduces hydroxy radicals produced by radiation, several radiation damage-reducing effects of hydrogen have been reported [9, 10]. Hirano *et al*. summarized the protective effects of hydrogen in animal models against various radiation injuries, including cognitive function, immune system, lung, cardiac, gastrointestinal, hematopoietic, testicular, skin, and cartilage disorders [10]. In most of these reports, hydrogen-rich solutions were used, which are easy to handle. Under normal atmospheric pressure, hydrogen is slightly soluble in water up to 0.8 mM (about 1.6 ppm, wt/vol); hydrogen gas is so small in molecules that it rapidly permeates the walls of glass and plastic containers, while aluminum walls can retain hydrogen gas for a relatively long time [9]. Technological advances to develop water with hydrogen trapped in smaller particles have enabled higher dissolved hydrogen concentrations and longer dissolution periods [11, 12]. Recently, we have developed a method to produce more stable hydrogen water by dispersing hydrogen in water using ultra-fine bubbles with a diameter of less than 1 μm [13,14]. These studies have reported the functional characteristics of long-life ultra-fine bubble hydrogen water (UBHW), which has excellent antioxidant activity and storage stability. UBHW is also expected to be used in medical applications to treat the onset and complications of lifestyle-related diseases, such as aging, arteriosclerosis, and diabetes, caused by oxidative stress, as well as radiation damage induced by ionizing radiation exposure. Its selective antioxidant properties against hydroxyl radicals, which are responsible for the indirect effects of ionizing radiation, may make it worthy of attention as a new radio-protector. However, the details of the action of UBHW in reducing radiation damage are not known, nor has a detailed assessment of the effects on biological components been carried out. In this study, we used a mouse model of severe acute radiation syndrome (ARS) that had been subjected to whole-body irradiation (WBI) with a lethal dose of X-rays and allowed them to consume UBHW *ad libitum* during feeding. The effectiveness of UBHW in mitigating radiation-induced damage was evaluated by 30-day survival rate and proteome analysis of the serum of surviving mice using liquid chromatography-tandem mass spectrometry (LC-MS/MS).

2. Materials and Methods

2.1. Ethical Statement

The institutional review board statement and approval number are listed in the "Institutional Review Board Statement" section. All efforts were made to minimize the number of animals used and their suffering in this study, which aligns with current animal welfare regulations.

2.2. Experimental **Design**

Seven-week-old female C57BL/6JJcl mice were delivered from the breeding facilities of CLEA Japan, Inc. (Tokyo, Japan). All mice were immediately housed in standard cages in a conventional clean room at an ambient temperature of 23°C with 50% relative humidity, and a 12 h light/dark cycle. These mice had *ad libitum* access to sterilized standard laboratory mouse chow and drinking water. Cages, chow, and drinking water were replaced with new ones weekly. We divided the mice into three groups that received different types of drinking water from each water bottle during the experiment, which were Hirosaki city tap water (TW), UBHW, or ultra-fine bubble oxygen water (UBOW), respectively. In addition, non-irradiated mice ingested TW were used as controls. The number of mice used in each experiment is indicated in the corresponding figure legends.

 doi:10.20944/preprints202408.0106.v1

2.3. Preparation of Ultra-Fine Bubble Water

Ultra-fine bubble water was prepared from deionized water according to our previous reports using a production system with resonant foaming and vacuum cavitation [13, 14].

2.4. In Vivo WBI with X-Rays

Eight-week-old mice were subjected to WBI with 6.0 Gy (sub-lethal dose) or 6.5 Gy (lethal dose) of X-rays (160 kV, 3 mA, 1.0 mm aluminum filter) at a dose rate of 0.622 Gy/min using an MX-160Labo (MediXtec, Chiba, Japan) with a distance of 300 mm between the focus and the target. The next section, "*In vitro irradiation with X-rays and electron spin resonance (ESR) spectroscopy*, was performed in a different laboratory, using an X-RAD iR-225 (Precision X-Ray, North Branford, CT, USA) to deliver 5 Gy of X-rays (200 kV, 15 mA, 1.0 mm aluminum filter) at a dose rate of 1.37 Gy/min.

2.5. In Vitro Irradiation with X-Rays and Electron Spin Resonance (ESR) Spectroscopy

Sample solutions were prepared by adding 10 uL of 1.0 M phosphate buffer (pH 7.4) and 4.5 uL of 22 mM 5,5-dimethyl-1-pyrroline-N-oxide (DMPO) aqueous solution adjusted with high-purity secondary distilled water (DW) to 885.5 uL of DW, TW, and UBHW, respectively. The sample is ultimately a solution of 100 μM DMPO and 1 mM phosphate buffer in each aqueous solvent. The samples were placed in 3 cm diameter plastic petri dishes and irradiated with 5 Gy of X-rays using an X-RAD iR-225. The amount of hydroxy radicals produced in the aqueous solution was 1.4 μM. Immediately after irradiation, the sample was transferred to a flat cell (60 × 10 × 0.25 mm) and X-band CW-EPR measurements were performed at ambient temperature using a JEOL-RE1X spectrometer (JEOL, Tokyo, Japan). The EPR parameters were as follows: incident microwave power, 10 mW; microwave frequency, 9.4335 GHz; modulation frequency, 100 kHz; field modulation amplitude, 0.1 mT; time constant, 0.1 min; scan range, 335.94 ± 5.0 mT; sweep time, 2 min/10 mT; receiver gain, 2.0×10^3. Relative EPR signal intensity was estimated using the signal of a co-mounted Mn^{2+} digital marker (ES-DM1, JEOL) in the cavity and Win-Rad software (Radical Research, Tokyo, Japan).

2.6. Serum Collection

Peripheral blood was harvested on day 30 after WBI from the orbital venous plexus of mice following anesthesia using isoflurane (Powerful Isoful; Zoetis, London, UK) by a capillary tube, and samples were left at room temperature for at least 30 min to allow for clotting. Serum was collected by centrifugation at 1200× g for 10 min and stored at −80 °C until the analysis.

2.7. Quantitative Analysis of 8-Hydroxydeoxyguanosine (8-OHdG)

The concentration of 8-OHdG in serum was analyzed using highly sensitive 8-OHdG check enzyme-linked immunosorbent assay (ELISA) monitoring kits (Jaica, Shizuoka, Japan) according to the manufacturer's protocols. Each assay was performed immediately after thawing of the serum sample. To remove high-molecular-weight proteins, which interfered with the analysis, each serum sample was filtered through an ultrafiltration membrane (molecular weight cut-off, 10 kDa; Nihon Pall, Ibaraki, Japan) before ELISA assay.

2.8. Liquid chromatography-Tandem Mass Spectrometry (LC-MS/MS)

The detailed measurement methods were described in our previous report [15]. In brief, serum was diluted with ammonium bicarbonate. The serum proteins were precipitated with acetone and resuspended in ammonium bicarbonate, at which point they were denatured with trifluoroethanol and dithiothreitol. Free cysteine residues were alkylated with iodoacetamide, which was quenched with dithiothreitol. The samples mixed with ammonium bicarbonate were incubated before trypsinization. These peptides were analyzed by LC-MS/MS using a nanoLC Eksigent 400 system coupled online to a TripleTOF 6600 mass spectrometer (AB Sciex; Framingham, MA, USA). A non-

 doi:10.20944/preprints202408.0106.v1

labeled quantitative method (SWATH) was used for the serum proteome analysis. Peptide peak areas were normalized to the sum of the peak areas of all measured peptides.

2.9. Identification of Differentially Expressed Proteins and Enrichment Analysis

The MetaboAnalyst 6.0 software package, which supports raw MS spectra processing, comprehensive data normalization, statistical analysis, functional analysis, and meta-analysis (https://www.metaboanalyst.ca, last accessed 4 June 2024), was used to compare the results of the differentially expressed proteins between WBI mice ingested TW or UBHW, respectively. A part of the data had missing values were removed and mean intensity centering was applied to the normalized peak area before the analyses. The expression profiles of proteins were compared based on the fold-change and unpaired Student's *t*-test with a cut-off *P* value of 0.05. Data were represented as the mean ± standard deviation (SD). A principal component analysis (PCA) and orthogonal partial least square-discriminant analysis (OPLS-DA) were performed for multivariate statistical analysis to determine the discriminated and predictive levels of the model. Results are visualized with the help of a volcano plot and heat map with dendrograms. The volcano plot was used to visualize the relationship between fold change and statistical significance, which showed that protein expression levels change as each plot moved away from the center; blue, red, and gray colors represent down-regulation, up-regulation, and no significant change, respectively. The heat maps show color-coded expression levels; color gradation from blue to red indicates low to high expression levels, respectively. Protein trees were drawn horizontally, and sample trees were drawn vertically. Gene ontology (GO) enrichment analyses of the differentially expressed proteins were performed using the Gene Ontology Resource (https://geneontology.org/, last accessed 4 June 2024). Expected shows the expected value, which is the number of genes you would expect in your list for this category, based on the reference list. Fold Enrichment shows the genes observed in the uploaded list over the expected (number in your list divided by the expected number). The Mouse Swiss-prot database was used as a reference set for the GO analyses. Bonferroni's correction was used for multiple tests.

2.10. Statistical Analyses

The levels of significance were calculated using the Excel 2016 software program (Microsoft, Redmond, WA, USA) with the Statcel 3 add-on (OMS, Saitama). *P* values of <0.05 were considered to indicate statistical significance by one-way ANOVA and Tukey-Kramer or Bonferroni/Dunn multiple comparison tests. A Kaplan-Meier analysis followed by a Mantel-Cox (log-rank) test was used to analyze the mouse survival rate.

3. Results

3.1. Survival of Mice Treated with Ultra-Fine Bubble Water Up To Day 30

After 6 Gy WBI, the 30-day survival rate of mice ingested TW *ad libitum* was approximately 37%. In contrast, the UBHW-treated group significantly suppressed WBI-induced lethality and the survival rate increased to 100% ($P = 0.0158$), and the UBOW-treated group increased their 30-day survival rate by 60% (Figure 1A). In the case of 6.5 Gy WBI, while the TW-treated group died out in about 3 weeks, the 30-day survival rate improved to 40% and 20% with UBHW intake or UBOW intake, respectively (Figure 1A). 8-OHdG is a known DNA oxidative damage marker in which the 8-position of deoxyguanosine, a base constituting DNA, is hydroxylated. Therefore, 8-OHdG in the peripheral blood of surviving mice subjected to WBI with 6.0 Gy of X-rays on day 30 was estimated (Figure 1B). When the hematocrit values at the time of blood collection were examined before 8-OHdG measurement, significant decrease was observed in all WBI groups compared to the control (47.6%), and these values recovered significantly more with UBHW intake (42.9%) than with TW (38.2%) or UBOW intake (32.3%). Serum 8-OHdG levels in mice that survived 30 days after WBI were significantly reduced by UBHW and UBOW intake compared to TW intake (Figure 1B). It was suggested that constant intake of UBHW or UBOW may reduce WBI-induced disability and lead to

 doi:10.20944/preprints202408.0106.v1

survival of mice, and in subsequent experiments, we focused on UBHW, which can have excellent life-saving effects on severe ARS mice.

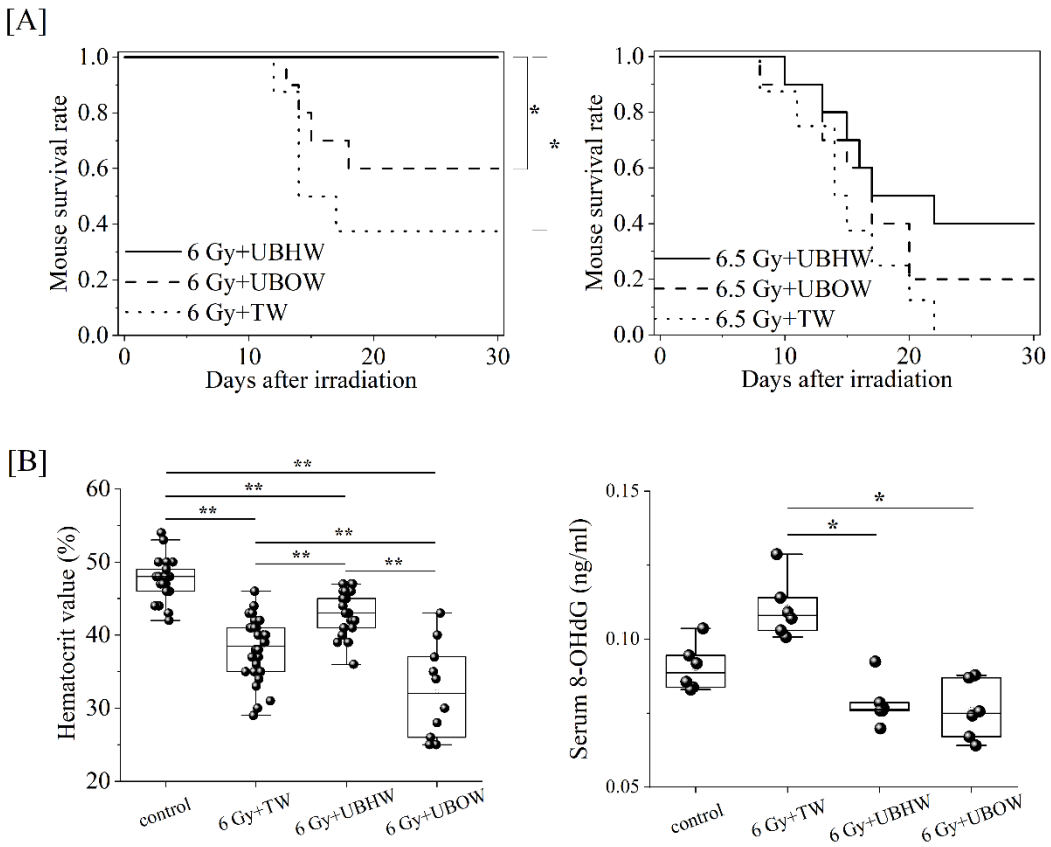

.

Figure 1. Radio-protective effect of each ultra-fine bubble water on TBI mice. (A) A Kaplan-Meier plot for the survival of 6 Gy or 6.5 Gy X-irradiated C57Bl/6JJcl female mice treated with UBHW (each n = 10), UBOW (each n = 10), or TW in Hirosaki (each n = 8), respectively. In addition, mice that were not subjected to TBI and only ingested tap water were used as controls. The statistical significance (*P* values of <0.05 (*)) of the difference was determined by a log-rank test. (B) Hematocrit values (%) and serum 8-OHdG levels (ng/ml) were shown. Statistically significant differences were evaluated by a one-way ANOVA and the multiple comparison tests; *P* values of <0.05 (*) or 0.01 (**).

3.2. Measurement of scavenging ability of UBHW against hydroxy radicals by ESR and spin-trapping technique

In water radiolysis, when DW is exposed to ionizing radiation, water molecules (H_2O) are known to decompose to form hydroxy radicals, hydrated electrons (e_{aq}^-), and hydrogen (H). Among these water radicals, hydroxy radicals are particularly reactive. When aqueous solutions containing the spin-trapping agent DMPO are irradiated with X-rays, the spin adduct DMPO-OH is specifically formed as shown in Figure 2A. This spin adduct has already been reported by an X-band electron spin resonance system to give a characteristic ESR spectrum with an intensity ratio of 1:2:2:1 due to the nuclear spins of the nitrogen atom (A_N = 1.49 mT) and hydrogen ($A_{H\beta}$ = 1.49 mT) at the β position of the trapping agent itself [16]. Suppose substance X in UBHW (X_{UBHW}), which competitively scavenges hydroxy radicals in this aqueous solution against DMPO, is present. In that case, a competitive reaction of the following reaction equation occurs and the intensity of the ESR spectrum in the absence of X_{UBHW} is attenuated depending on the concentration of X and the reaction rate. $k_{(DMPO+OH)}$ was reported as 3.4×10^9 $M^{-1}{\cdot}s^{-1}$ [17].

DMPO + OH → DMPO-OH ($V_1 = k_{(DMPO+OH)}$ [DMPO][OH])

X_{UBHW} + OH → products ($V_2 = k_{(X+OH)}$ [X_{UBHW}][OH])

 doi:10.20944/preprints202408.0106.v1

ESR spectra obtained from similar irradiation experiments with TW are shown in the black ESR spectrum of Figure 2A. The signal intensity showed little change compared to that obtained with DW (the green ESR spectrum). On the other hand, the signal intensity in similar irradiation experiments with UBHW, shown in the red ESR spectrum, was significantly reduced to about half that of DW. The relative signal intensities of TW and UBHW were plotted, with the signal intensity of the OH adduct as Hs shown in the green ESR spectrum of Figure 2A, standardized by the signal intensity $H_{Mn^{2+}}$ of the Mn^{2+} digital marker, which was always set to the same condition, with DW on each day as 1.0. In comparison with the signal intensity of DW, that of TW did not show any significant decrease in signal intensity from the beginning of the experiment to 32 days, while that of UBHW was found to have decreased from 50% to 40% as shown in Figure 2B. During this experimental period, all samples were stored in the same refrigerator at 4°C under identical conditions. These results suggest that UBHW contains substances that scavenge hydroxy radicals. The most likely candidate is hydrogen gas, but the reaction rate between hydrogen gas and hydroxy radicals is already known to be $k_{(H2+OH)} = 4.0 \times 10^7\ M^{-1}{\cdot}s^{-1}$ [18]. From the reaction kinetics equation, $k_{(DMPO+OH)}[DMPO][OH] = k_{(H2+OH)}[H_2][OH]$ for 50% [OH] to react with hydrogen gas, which should be $[H_2] = 8.5$ mM. The solubility of hydrogen gas in water at 20°C is about 0.81 mM [9]. By creating ultra-fine bubbles, it is possible to confine high concentrations of hydrogen to an order of magnitude higher concentration, which is thought to increase the scavenging activity of hydroxy radicals. Our previous paper showed that the low level of the oxidation-reduction potential and the high scavenging capacity of 1,1-diphenyl-2-picrylhydrazyl (DPPH) radicals in UBHW were maintained for as long as three months [14], and the present experiments also showed that the radiation-induced hydroxy radical scavenging ability was maintained for more than one month. This means that the ultra-fine bubbles remain in the bottle for more than a month after they are produced. We evaluated how long the ultra-fine bubbles would remain in the bottle by irradiating the sealed polyethylene terephthalate container in which the sample was stored with green laser light (532 nm) with 1 mW power, which is commonly used as a pointer, and visually observing the scattered light in a dark room, as shown in Figure 2C. The images of the laser irradiation of DW and UBHW shown in Figure 2D clearly show that the scattered light originating from the ultra-fine bubbles is present in UBHW for at least one month after its production, at least as long as it was present immediately after production. Nirmalkar *et al.* have already reported that nanobubbles maintain their bubble size and number for 6 months [19], and the present results reaffirm this property of nanobubbles.

Preprints.org (www.preprints.org) | NOT PEER-REVIEWED | Posted: 1 August 2024 doi:10.20944/preprints202408.0106.v1

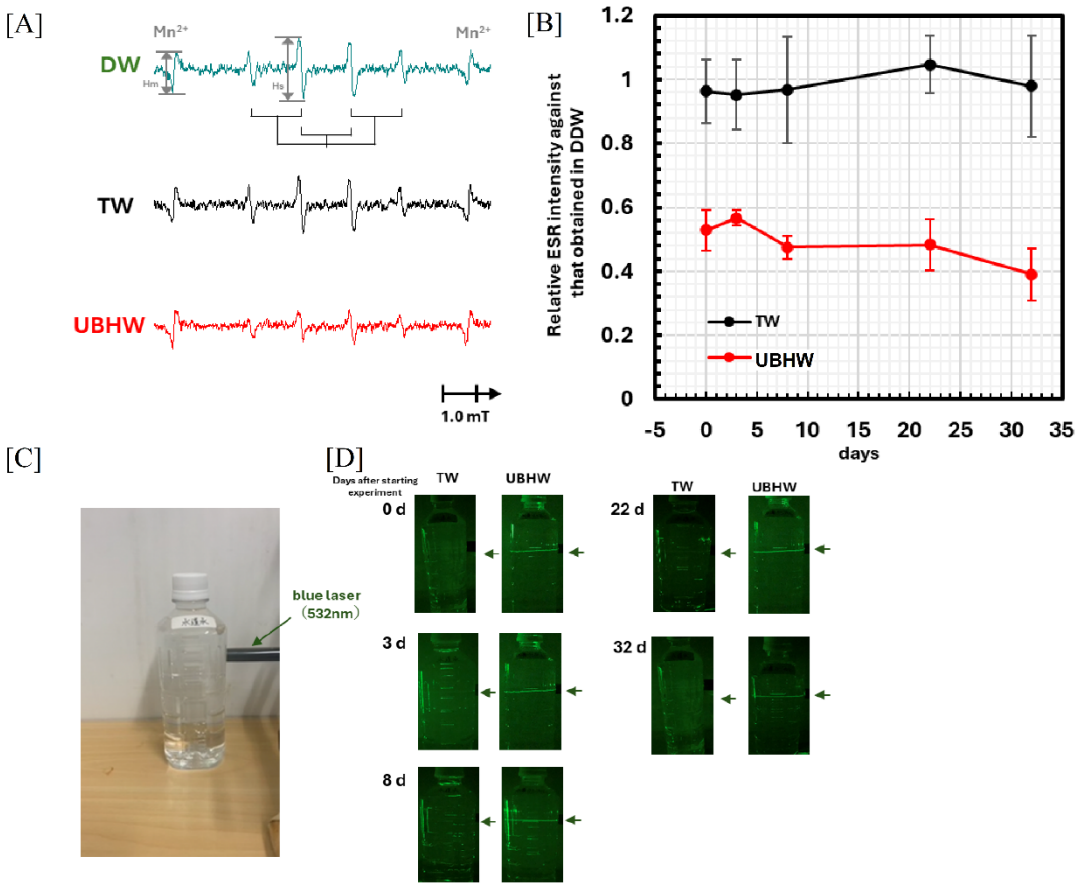

Figure 2. Measurement of scavenging ability of UBHW against hydroxy radicals. (A) The ESR spectrum immediately after DW (green line), TW (black line), and UBHW (red line) containing 100 uM DMPO and 1 mM potassium phosphate (pH 7.4) were irradiated with 5 Gy, respectively. (B) Time course of the relative signal intensity of the ESR spectra, where the relative values of h_s/h_{Mn2+} obtained in TW and UBHW are plotted when the h_s/hMn_{2+} in DW is standardized to 1.0. Three independent experiments were performed. Each point and vertical bar represents the mean ± SD. Statistical treatment was performed by Student's t-test for DW data, indicated by * when $P < 0.05$ and ** when $P < 0.01$. (C and D) The lifetime of the nanobubbles in the UBHW was conventionally confirmed by means of a laser pointer (532 nm) with 1 mW. The bottles were irradiated under the same conditions as shown in C at the time of the date noted from the first experiment to visualize the side scattering light. The photographs were taken in a dark room as shown in D.

3.3. Proteome analysis of mice treated with UBHW

LC-MS/MS was used to examine the expression of serum proteins of mice consistently ingested UBHW or TW, respectively, on day 30 after WBI with a sub-lethal dose of X-rays, because lethal WBI of TW-fed mice results in the death of all mice. In order to elucidate the mechanism through which UBHW alleviates radiation damage, the full dataset from all mouse serum samples was subjected to a PCA to obtain an overview of the data. The first and second principal component scores were 18.7% and 16.7%, respectively. A plot of the first two principal component scores, which accounted for 35.4% of the original variation, is shown in Figure 3A (the ellipse represents a 95% tolerance region for the scores based on Hotelling's T2). There are no major outliers. An OPLS-DA was applied to the samples to visualize class separation. The OPLS-DA model concentrates all of the discriminating information into the first component. The score scatter plots of the OPLS-DA model in Figure 3B demonstrated satisfactory separation between mice constantly ingested UBHW or TW, respectively,

 doi:10.20944/preprints202408.0106.v1

using one predictive component and one orthogonal component, which were completely separated along the first predictive component. These results indicate that the serum proteomic profile can be used to distinguish UBHW-treated mice from TW-treated mice.

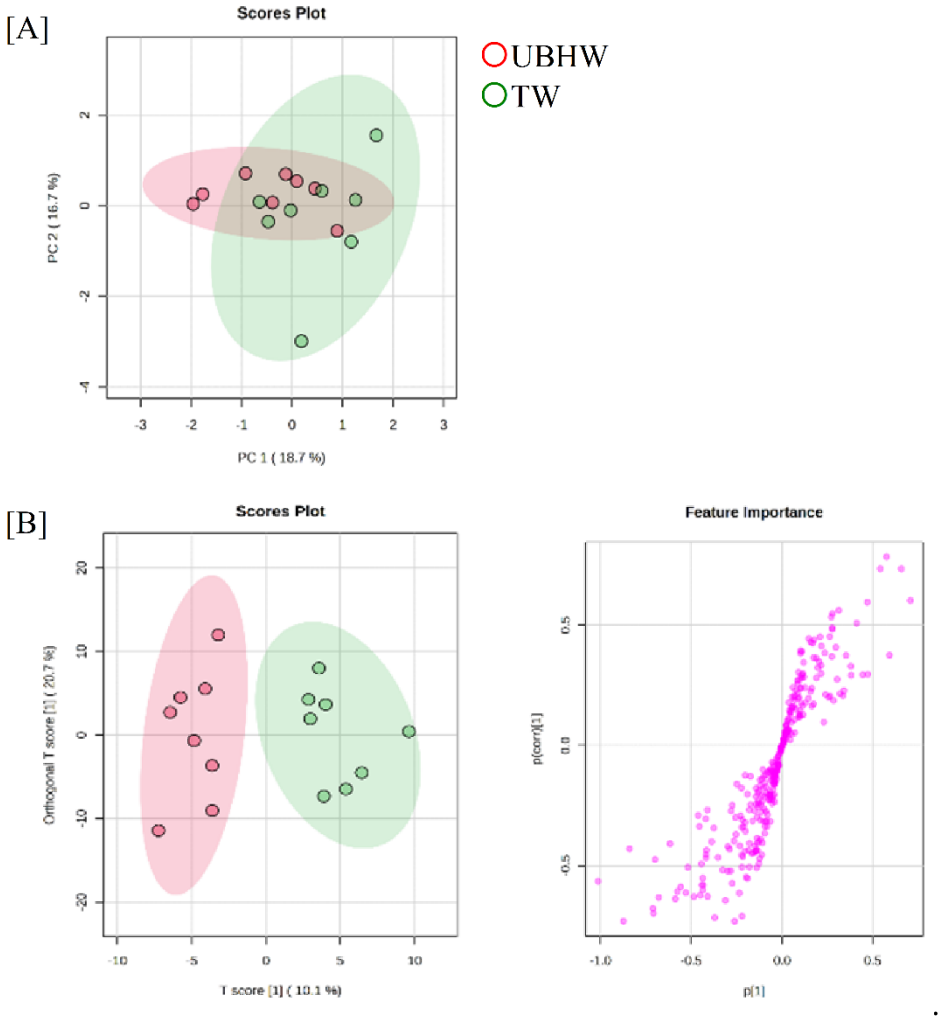

Figure 3. Proteomic analysis of serum from mice constantly ingested UBHW. (A) A PCA overview of all 16 mice serum samples (n = 8 per each group). Uncharacterized samples are plotted at the center, and those with features are plotted at a distance from the center. Similar features are plotted at close positions. (B) Score scatter plots of the OPLS-DA model based on serum proteome data. A score scatter plot (left panel) and S-plot (right panel) are represented. The ellipse in each score scatter plot indicates the Hotelling T2 (0.95) range for this model. Red or green circles mean mice treated with UBHW or TW, respectively.

This analysis revealed a total of 326 differentially expressed proteins upon radiation exposure while ingesting UBHW, including 164 up-regulated and 162 down-regulated proteins, and after univariate Student's *t*-test data processing, 26 (17 were up-regulated and 9 were down-regulated) proteins with a significant change in expression in UBHW relative to TW are extracted, as represented in the volcano plot (Figure 4A). A hierarchical cluster analysis demonstrated that proteins in the UBHW-treated mice could be distinguished from that in the TW-treated mice based on their protein expression patterns, which showed the variation in 14 responsive proteins identified by Student's t-test with a cut-off *P* value of 0.05 (Figure 4B).

 doi:10.20944/preprints202408.0106.v1

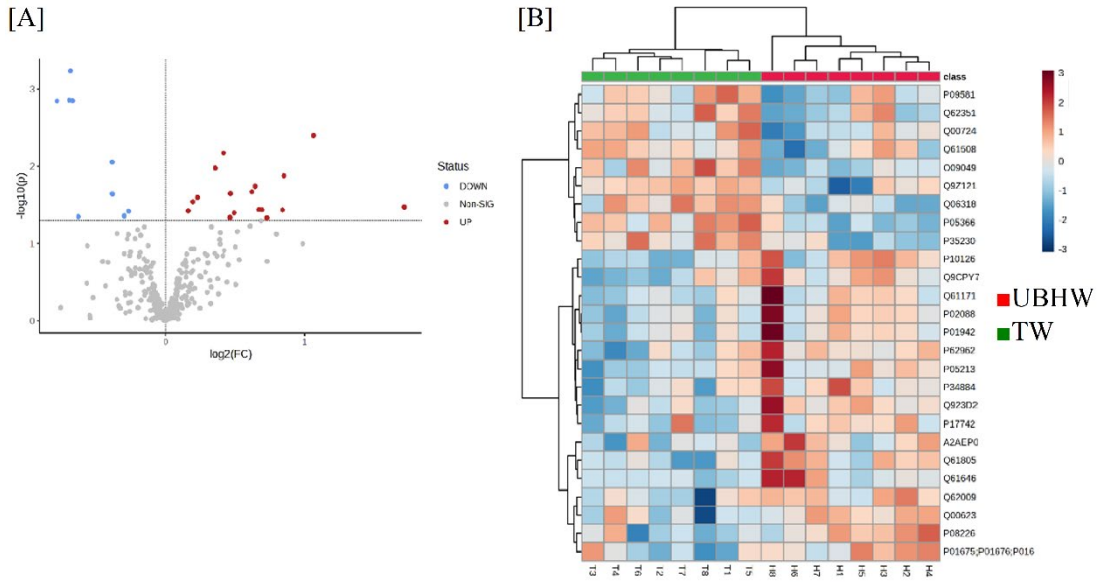

.

Figure 4. Identification of differentially expressed serum proteins of mice constantly ingested UBHW. (A) In the volcano plot, the vertical lines correspond to a 1.0-fold increase or decrease in an expression level, while the horizontal line represents a *P* value of 0.05. Gray points in the plot represent proteins with no statistical differences, and red/blue points represent significantly up-regulated/down-regulated proteins, respectively. (B) A heat map with dendrograms showed the variation in 14 responsive proteins out of 326 serum proteins, which were identified by Student's t-test with a cut-off *P* value of 0.05, using the MetaboAnalyst 5.0 software package.

Twenty-six proteins were listed by UniProt ID, protein name, *P* value, and fold-change, based on the MetaboAnalyst 6.0 software package (Table 1). A statistical analysis with GO based on the biological process criterion revealed that 17 up-regulated serum proteins due to a daily intake of UBHW were related to the "positive regulation of phospholipid efflux" and "hydrogen peroxide catabolic process", and Reactome pathway analysis showed that these proteins were involved in the "scavenging by class A receptors", "HDL remodeling", "chylomicron assembly", "chylomicron remodeling", and "cellular response to stress" (Table 2). These results suggest that these processes may be related to a response to UBHW. On the other hand, a statistical analysis with GO based on the biological process criterion revealed that 9 down-regulated serum proteins due to a daily intake of UBHW were related to the "inflammatory response", "regulation of cell population proliferation", "regulation of immune system process", and "response to organic substance", but Reactome pathway analysis showed no corresponding functions (Table 3).

Table 1. Candidate significant differentially expressed serum protein list.

No.	UniProt ID	Gene name	Protein name	FC	*P*
1	Q61646	*Hp*	Haptoglobin	3.287	0.034
2	Q923D2	*Blvrb*	Flavin reductase	2.090	0.004
3	P02088	*Hbb-b1*	Hemoglobin subunit beta-1	1.803	0.013
4	P01942	*Hba*	Hemoglobin subunit alpha	1.790	0.037
5	Q61171	*Prdx2*	Peroxiredoxin-2	1.656	0.046
6	P34884	*Mif*	Macrophage migration inhibitory factor	1.616	0.037
7	A2AEP0	*Obp1b*	Odorant-binding protein 1b	1.592	0.036
8	P10126	*Eef1a1*	Elongation factor 1-alpha 1	1.562	0.018
9	P62962	*Pfn1*	Profilin-1	1.536	0.021
10	P05213	*Tuba1b*	Tubulin alpha-1B chain	1.406	0.040
11	P01675	–	Ig kappa chain V-VI region XRPC 44	1.380	0.022

 doi:10.20944/preprints202408.0106.v1

12	P17742	*Ppia*	Peptidyl-prolyl cis-trans isomerase A	1.377	0.046
13	Q61805	*Lbp*	Lipopolysaccharide-binding protein	1.334	0.007
14	P08226	*Apoe*	Apolipoprotein E	1.280	0.010
15	Q62009	*Postn*	Periostin	1.172	0.025
16	Q00623	*Apoa1*	Apolipoprotein A1	1.144	0.029
17	Q9CPY7	*Lap3*	Cytosol aminopeptidase	1.119	0.038
18	Q61508	*Ecm1*	Extracellular matrix protein 1	0.831	0.038
19	P09581	*Csf1r*	Macrophage colony-stimulating factor 1 receptor	0.812	0.044
20	Q00724	*Rbp4*	Retinol-binding protein 4	0.766	0.023
21	Q9Z121	*Ccl8*	C-C motif chemokine 8	0.765	0.009
22	Q62351	*Tfrc*	Transferrin receptor protein 1	0.646	0.045
23	O09049	*Reg3g*	Regenerating islet-derived protein 3-gamma	0.628	0.001
24	P05366	*Saa1*	Serum amyloid A-1 protein	0.622	0.001
25	Q06318	*Scgb1a1*	Uteroglobin	0.618	0.001
26	P35230	*Reg3b*	Regenerating islet-derived protein 3-beta	0.581	0.001

Note. P value determined by a *t*-test, FC: Fold change in comparison to TW-treated mice.

Table 2. The GO enrichment and Reactome pathway analysis of identified up-regulated proteins.

	Mus musculus (References)	Significant proteins	Expected	Fold enrichment	*P* value
GO biological process complete					
positive regulation of phospholipid efflux	4	Q00623, P08226	0.00	> 100	0.0314
hydrogen peroxide catabolic process	27	P02088, Q61171, P01942	0.02	> 100	0.0103
Reactome pathways					
scavenging by class A receptors	8	Q00623, P08226	0.01	> 100	0.0265
HDL remodeling	9	Q00623, P08226	0.01	> 100	0.0341
chylomicron assembly	10	Q00623, P08226	0.01	> 100	0.0426
chylomicron remodeling	10	Q00623, P08226	0.01	> 100	0.0426
cellular responses to stress	451	P10126, P05213, Q923D2, Q61171, P01942, Q00623	0.35	17.20	0.0012

4. Discussion

The present study examined that UBHW was administered *ad libitum* to mice treated with WBI, and the function of UBHW was evaluated by 30-day survival rate and proteomic analysis of serum from surviving individuals. The 30-day survival rate of 6 Gy WBI mice ingested with UBHW increased to 100% with lethality significantly reduced in the TW-treated group from approximately 37% of controls (Figure 1A). In contrast, the UBOW intake group improved to 60% (no significant difference). The main cause of radiation-induced biological effects is ROS and free radicals, such as hydroxy radicals, superoxide anion, and hydrogen peroxide, which are generated by ionization and excitation of water molecules in living organisms. This is called indirect action, as distinguished from

 doi:10.20944/preprints202408.0106.v1

the direct action of radiation on biomolecules. Previous studies have consistently demonstrated the radiation damage-reducing effects of hydrogen. Qian *et al*. examined the radioprotective properties of hydrogen water and demonstrated its ability to reduce radiation-induced oxidative stress [20]. Guo *et al.* found that hydrogen treatment diminished the detrimental effects of low-dose long-term radiation in mice [21], while Qiu *et al.* showed that hydrogen attenuated radiation-induced intestinal damage by reducing oxidative stress and inflammatory response [22]. Furthermore, Ohsawa *et al*. reported that the inhalation of hydrogen gas ameliorated ischemia-reperfusion injury in a rat model with cerebral infarction [3]. This report showed that hydrogen is an antioxidant that selectively reduces highly oxidative ROS and reactive nitrogen species, such as hydroxy radicals and peroxynitrite, but does not react with other ROS, such as superoxide anion and hydrogen peroxide. Therefore, it is suggested that UBHW may have shown a survival effect in mice treated with sub-lethal WBI due to the selective reduction of hydroxy radicals and peroxynitrite by hydrogen. In addition, the present study used the ESR method to show that the amount of hydroxy radicals produced by X-irradiation of UBHW is significantly lower than in control TW (Figure 2A and 2B). In particular, these hydroxy radicals scavenging capacity was also demonstrated by the ESR methods to be maintained for at least one month after its production during the periods in survival assessment of WBI mice (Figure 1A), suggesting that UBHW contains substances that scavenge hydroxy radicals and these activities are maintained for a long period.

Table 3. The GO enrichment and Reactome pathway analysis of identified down-regulated proteins.

	Mus musculus (References)	Significant proteins	Expected	Fold enrichment	*P* value
GO biological process complete					
inflammatory response	544	O09049, P09581, Q9Z121, P35230, Q61508	0.20	25.68	0.0044
regulation of cell population proliferation	1786	O09049, P09581, Q62351, P35230, Q00724, Q61508, Q06318	0.65	10.77	0.0016
regulation of immune system process	1661	O09049, P09581, Q62351, Q00724, Q61508, Q06318	0.60	9.93	0.0421
response to organic substance	2499	O09049, P09581, Q9Z121, Q62351, P35230, Q00724, Q06318	0.91	7.70	0.0163

Accidental exposure to high doses of radiation, such as nuclear disasters and radiation accidents, can result in death from ARS due to myelosuppression and intestinal disorders [21, 22]. Appropriate treatment should therefore be given immediately after radiation exposure. Bone marrow transplantation is available for recovery from radiation-induced bone marrow damage. Still, bone

 doi:10.20944/preprints202408.0106.v1

marrow transplantation for radiation accident victims has several limitations, including histocompatibility, age constraints, human leukocyte antigen type, and the need for immunosuppression to reduce the risk of graft-versus-host rejection. In contrast, pharmacological approaches can accommodate large numbers of victims with few limitations. Radioprotective agents are generally classified into four categories based on their mechanism of action: radical scavengers, agents that activate biological defense mechanisms, agents that prevent systemic absorption and deposition, and agents that promote the excretion of radionuclides [23]; the UBHW introduced here is thought to function mainly as a radical scavenger. Amifostine (WR2721) has been developed as a radioprotective agent with free radical scavenging properties, such as against hydroxy radicals. It is the only radioprotective agent approved by the U.S. Food and Drug Administration for clinical use [24-29]. However, this drug has not been widely considered a useful radioprotective agent of choice because of its dose-dependent side effects such as hypotension, nausea, and vomiting [27]. Hirano *et al*. recently showed that although hydrogen is an inactive substance, compared to other antioxidants, it is the only molecule with mitochondrial permeability and the ability to reduce hydroxy radicals, which is promising for future medical applications [30, 31]. They suggested that selective hydroxy radicals scavengers may have potential medical applications as radioprotective agents.

The present study showed that a total of 326 differentially expressed proteins were found in the analysis of serum proteins on day 30 of individuals surviving UBHW ingestion in WBI mice. Of these, 26 proteins were extracted whose expression was significantly altered in UBHW compared to TW, 17 of which were up-regulated and 9 down-regulated (Figure 3A). A common function of the up-regulated proteins involves a wide range of biological functions, including immune response, energy generation, and cellular movement. Haptoglobin, for example, is involved in host defense responses to infection and inflammation [32], while Flavin reductase is important for the function of hemostatic proteins [33]. Hemoglobin subunit beta-1 and Hemoglobin subunit alpha are part of the respiratory pigments of mammals and some invertebrates, with the ability to bind ligands and undergo redox changes. Macrophage migration inhibitory factor and lipopolysaccharide-binding protein, play a role in the innate immune system [34]. These proteins collectively contribute to the proper functioning of a living cell, highlighting their significance in various biological processes. Regarding the down-regulated proteins, the common functions are role in promoting tissue degradation, inflammation, and tumor progression [35]. These proteins can also trigger the formation of disease-specific harmful products in neurodegenerative disorders [36]. Furthermore, they can influence leukocyte function, particularly in the production of inflammatory mediators and cytokines [37]. In addition, bioinformatics analysis reveals that the regulation of phospholipid efflux is a crucial function that helps maintain cellular homeostasis and prevent the accumulation of harmful lipids. Similarly, the hydrogen peroxide catabolic process, which involves the scavenging of hydrogen peroxide by class A receptors, plays a key role in cellular regulation and stress response [38]. HDL remodeling, chylomicron assembly, and chylomicron remodeling are all involved in lipid metabolism and transport, with HDL also exhibiting anti-inflammatory properties. Lastly, cellular responses to stress, including the regulation of redox balance, are influenced by the beneficial effects of molecular hydrogen [39]. Therefore, it is suggested that UBHW may enhance and regulate these functions, resulting in reduced damage in mice treated with sub-lethal dose WBI.

In conclusion, the present study demonstrated that hydrogen water, particularly in the form of UBHW, has potential applications in reducing radiation damage. However, further research is needed to fully understand the mechanisms and potential challenges of using UBHW as a radiation damage mitigator.

Author Contributions: I.K. and M.H designed and managed the study; M.Y., Y.T., Y.S., C.K., O.I. and I.K. performed the experiments; M.Y., K.T.H., O.I. and I.K. wrote this manuscript. All authors contributed extensively to discussions regarding the work and the review of the manuscript.

Funding: This work was partially supported by a KAKENHI Grant-in-Aid for Scientific Research (B) (No. 21H02860 IK) and by a KAKENHI Grant-in-Aid for Young Scientists (No. 21K17887 MY).

Institutional Review Board Statement: The study was approved by the animal experiment committee of Hirosaki University (approval number: G17001).

 doi:10.20944/preprints202408.0106.v1

Informed Consent Statement: Not applicable.

Data Availability Statement: Data are contained within the article.

Acknowledgments: The authors are grateful to Miyu Miyazaki at the Center for Scientific Equipment Management, Hirosaki University Graduate School of Medicine, for helping with the LC-MS/MS analysis.

Conflicts of Interest: The authors declare they have no actual or potential competing financial interests.

References

1. Zhang, J.; Shim, G.; de Toledo, SM.; Azzam, E.I. The translationally controlled tumor protein and the cellular response to ionizing radiation-induced DNA damage. *Results Probl Cell Differ* **2017**, *64*, 227-253. doi: org/10.1007/978-3-319-67591-6_12.
2. Helm, J.S.; Rudel, R.A. Adverse outcome pathways for ionizing radiation and breast cancer involve direct and indirect DNA damage, oxidative stress, inflammation, genomic instability, and interaction with hormonal regulation of the breast. *Arch Toxicol* **2020**, *94*, 1511-1549. doi: org/10.1007/s00204-020-02752-z.
3. Ohsawa, I.; Ishikawa, M.; Takahashi, K.; Watanabe, M.; Nishimaki, K.; Yamagata, K.; Katsura, K.; Katayama, Y.; Asoh, S.; Ohta, S. Hydrogen acts as a therapeutic antioxidant by selectively reducing cytotoxic oxygen radicals. *Nat Med* **2017**, *13*, 688-694 (2017). doi: org/10.1038/nm1577.
4. Dohi, K.; Satoh, K.; Miyamoto, K.; Momma, S.; Fukuda, K.; Higuchi, R.; Ohtaki, H.; Banks, WA. Molecular hydrogen in the treatment of acute and chronic neurological conditions: mechanisms of protection and routes of administration. *J Clin Biochem Nutr* **2017**, *61*, 1-5. doi: 10.3164/jcbn.16-87.
5. Zhang, Y.; Tan, S.; Xu, J.; Wang, T. Hydrogen therapy in cardiovascular and metabolic diseases: from bench to bedside. *Cell Physiol Biochem* **2018**, *47*, 1-10. doi: 10.1159/000489737.
6. Matei, N.; Camara, R.; Zhang, J.H. Emerging mechanisms and novel applications of hydrogen gas therapy. *Med Gas Res* **2018**, *8*, 98-102. doi: 10.4103/2045-9912.239959.
7. Li, H.; Luo, Y.; Yang, P.; Liu, J. Hydrogen as a complementary therapy against ischemic stroke: A review of the evidence. *J Neurol Sci* **2019**, *396*, 240-246. doi: 10.1016/j.jns.2018.11.004.
8. Sano, M.; Tamura, T. Hydrogen Gas Therapy: From Preclinical Studies to Clinical Trials. *Curr Pharm Des* **2021**, *27*, 650-658. doi: 10.2174/1381612826666201221150857.
9. Hu, Q.; Zhou, Y.; Wu, S.; Wu, W.; Deng, Y.; Shao, A. Molecular hydrogen: A potential radioprotective agent. *Biomed Pharmacother* **2020**, *130*, 110589. doi: 10.1016/j.biopha.2020.110589.
10. Hirano, S.I.; Ichikawa, Y.; Sato, B.; Yamamoto, H.; Takefuji, Y.; Satoh, F. Molecular hydrogen as a potential clinically applicable radioprotective agent. *Int J Mol Sci* **2021**, *22*, 4566. doi: 10.3390/ijms22094566.
11. Liu, S.; Oshita, S.; Thuyet, D.Q.; Saito, M.; Yoshimoto, T. Antioxidant activity of hydrogen nanobubbles in water with different reactive oxygen species both in vivo and in vitro. *Langmuir* **2018**, *34*, 11878-11885. doi: org/10.1021/acs.langmuir.8b02440.
12. Zhang, Y.; Fan, W.; Li, X.; Wang, W.X.; Liu, S. Enhanced removal of free radicals by aqueous hydrogen nanobubbles and their role in oxidative stress. *Environ Sci Technol* **2022**, *56*, 15096-15107. doi: org/10.1021/acs.est.2c03707.
13. Unites States Patent. Available online: https://image-ppubs.uspto.gov/dirsearch-public/print/downloadPdf/10500553 (accessed on 12 May 2024).
14. Kamimura, C.; Ohba, R.; Yamaguchi, M.; Hosoda, M.; Kashiwakura, I. Functional characteristics of antioxidant long-life ultra-fine bubble hydrogen water. *Inorganics* **2024**, *12*, 141. doi: org/10.3390/inorganics12050141.
15. Yamaguchi, M.; Tatara, Y.; Nugraha, E.D.; Ramadhani, D.; Tamakuma, Y.; Sato, Y.; Miura, T.; Hosoda, M.; Yoshinaga, S.; Syaifudin, M.; Kashiwakura, I.; Tokonami, S. Detection of biological responses to low-dose radiation in humans. *Free Radic Biol Med* **2022**, *184*, 196-207. doi: 10.1016/j.freeradbiomed.2022.04.006.
16. Buettner, G.R. Spin trapping: ESR parameters of spin adducts. *Free Radic Biol Med* **1987**, *3*, 259-303. doi: 10.1016/s0891-5849(87)80033-3.
17. Finkelstein, E.; Rosen, G.M.; Rauckman, E.J. Spin trapping of superoxide and hydroxyl radical: practical aspects. *Arch Biochem Biophys* **1980**, *200*, 1-16. doi: 10.1016/0003-9861(80)90323-9.
18. Farhataziz, Ross, A.B. Selected specific rates of reactions of transients from water in aqueous solution. III. Hydroxyl radical and perhydroxyl radical and their radical ions. *NSRDS-NBS* **1977**, *59*, 126.
19. Nirmalkar, N.; Pacek, A.W.; Barigou, M. On the Existence and Stability of Bulk Nanobubbles. *Langmuir* **2018**, *34*, 10964-10973. doi: 10.1021/acs.langmuir.8b01163.
20. Qian, L.; Shen, J.; Chuai, Y.; Cai, J. Hydrogen as a new class of radioprotective agent. *Int J Biol Sci* **2013**, *9*, 887-894. doi: 10.7150/ijbs.7220.
21. Guo, J.; Zhao, D.; Lei, X.; Zhao, H.; Yang, Y.; Zhang, P.; Liu, P.; Xu, Y.; Zhu, M.; Liu, H.; Chen, Y.; Chuai, Y.; Li, B.; Gao, F.; Cai, J. Protective Effects of Hydrogen against Low-Dose Long-Term Radiation-Induced Damage to the Behavioral Performances, Hematopoietic System, Genital System, and Splenic Lymphocytes in Mice. *Oxid Med Cell Longev* **2016**, *2016*, 1947819. doi: 10.1155/2016/1947819.

22. Qiu, X.; Dong, K.; Guan, J.; He, J.M. Hydrogen attenuates radiation-induced intestinal damage by reducing oxidative stress and inflammatory response. *Int Immunopharmacol* **2020**, *84*, 106517. doi: 10.1016/j.intimp.2020.106517.
23. Guan, B.; Li, D.; Meng, A. Development of radiation countermeasure agents for acute radiation syndromes. *Animal Model Exp Med* **2023**, *6*, 329-336. doi: 10.1002/ame2.12339.
24. Ji, L.; Cui, P.; Zhou, S.; Qiu, L.; Huang, H.; Wang, C.; Wang, J. Advances of Amifostine in Radiation Protection: Administration and Delivery. *Mol Pharm* **2023**, *20*, 5383-5395. doi: 10.1021/acs.molpharmaceut.3c00600.
25. King, M.; Joseph, S.; Albert, A.; Thomas, T.V.; Nittala, M.R.; Woods, W.C.; Vijayakumar, S.; Packianathan, S. Use of Amifostine for Cytoprotection during Radiation Therapy: A Review. *Oncology* **2020**, *98*, 61-80. doi: 10.1159/000502979.
26. Bahat, Z.; Cobanoglu, U.; Ulku, C.; Kalyoncu, N.İ.; Caner, K.S.; Yavuz, M.N. Could Amifostine Prevent Experimental Radiotherapy-Induced Acute Pericarditis? *Asian Pac J Cancer Prev* **2022**, *23*, 3209-3213. doi: 10.31557/APJCP.2022.23.9.3209.
27. Koukourakis, M.I.; Maltezos, E. Amifostine administration during radiotherapy for cancer patients with genetic, autoimmune, metabolic and other diseases. *Anticancer Drugs* **2006**, *17*, 133-138. doi: 10.1097/00001813-200602000-00003.
28. Kouvaris, J.R.; Kouloulias, V.E.; Vlahos, L.J. Amifostine: the first selective-target and broad-spectrum radioprotector. *Oncologist* **2007**, *12*, 738-747. doi: 10.1634/theoncologist.12-6-738.
29. Wasserman, T.H.; Brizel, D.M. The role of amifostine as a radioprotector. *Oncology (Williston Park)* **2001**, *15*, 1349-1354.
30. Hirano, S.I.; Ichikawa, Y.; Kurokawa, R.; Takefuji, Y.; Satoh, F.A. "philosophical molecule," hydrogen may overcome senescence and intractable diseases. *Med Gas Res* **2020**, *10*, 47-49. doi: 10.4103/2045-9912.279983.
31. Hirano, S.; Ichikawa, Y.; Sato, B.; Satoh, F.; Takefuji, Y. Hydrogen is promising for medical applications. *Clean Technol* **2020**, *2*, 529-541. doi: 10.3390/cleantechnol2040033.
32. Dobryszycka, W. Biological functions of haptoglobin--new pieces to an old puzzle. *Eur J Clin Chem Clin Biochem* **1997**, *35*, 647-654.
33. Karlaftis, V.; Perera, S.; Monagle, P.; Ignjatovic, V. Importance of post-translational modifications on the function of key haemostatic proteins. *Blood Coagul Fibrinolysis* **2016**, *27*, 1-4. doi: 10.1097/MBC.0000000000000301.
34. Beishuizen, A.; Thijs, L.G.; Haanen, C.; Vermes, I. Macrophage migration inhibitory factor and hypothalamo-pituitary-adrenal function during critical illness. *J Clin Endocrinol Metab* **2011**, *86*, 2811-2816. doi: 10.1210/jcem.86.6.7570.
35. Labat-Robert, J. Cell-matrix interactions in aging: role of receptors and matricryptins. *Ageing Res Rev* **2004**, *3*, 233-247. doi: 10.1016/j.arr.2003.10.002.
36. Pintér, P.; Alpár, A. The Role of Extracellular Matrix in Human Neurodegenerative Diseases. *Int J Mol Sci* **2022**, *23*, 11085. doi: 10.3390/ijms231911085.
37. Pakianathan, D.R. Extracellular matrix proteins and leukocyte function. *J Leukoc Biol* **1995**, *57*, 699-702. doi: 10.1002/jlb.57.5.699a.
38. Rhee, S.G.; Chang, T.S.; Bae, Y.S.; Lee, S.R.; Kang, S.W. Cellular regulation by hydrogen peroxide. *J Am Soc Nephrol* **2003**, *14*, S211-215. doi: 10.1097/01.asn.0000077404.45564.7e.
39. Radyuk, S.N. Mechanisms Underlying the Biological Effects of Molecular Hydrogen. *Curr Pharm Des* **2021**, *27*, 626-735. doi: 10.2174/1381612826666201211112846.